Surface Science 130 (1983) 124–154
North-Holland Publishing Company

AVERAGED LOCAL FIELD INTENSITIES IN COMPOSITE FILMS

Zvi KOTLER and Abraham NITZAN

Department of Chemistry, Tel Aviv University, Tel Aviv 69978, Israel

Received 28 December 1982

The photophysical properties of molecules adsorbed in composite films (e.g. surface island films) depend on the local electromagnetic field within the film. The ratio between the average field intensity $\langle|E|^2\rangle$ in the film and the intensity $|E_l|^2$ associated with the incident field is a measure of the electromagnetic contribution to the surface influence on molecular photophysical phenomena. This ratio depends on the film composition and morphology, on the dielectric properties of the pure components making the film and on the frequency, direction and polarization of the incident radiation. Calculations of this ratio as a function of these parameters for several models of composite films are presented. Image interactions and retardation effects as well as radiative damping and finite size contributions to the dielectric response of the films are taken into account. In addition, an estimate of the field inhomogeneity within the film is obtained by calculating also the ratio $\langle|E|^2\rangle_{\text{shell}}/|E_l|^2$ associated with the field in thin shells surrounding the dielectric particles which constitute the film.

1. Introduction

Much attention has been focussed recently on optical processes associated with molecules adsorbed on rough dielectric surfaces or on island films [1,2]. Surface enhanced Raman scattering (SERS) [1] is perhaps the most pronounced example, however the proximity of the surface may affect any observable electromagnetic property of the adsorbed molecule [2].

While it seems that electron transfer interactions contribute to the observed surface induced modification of molecular optical properties [3], there is little doubt that a major contribution comes from the fact that the electromagnetic field itself is modified near the interface [4]. Recent works study this effect for an isolated dielectric spheroid [4a], an aggregate of two spheres 4b] or for a sinosoidal grating [4c]. The simple geometries considered in these works make it possible to obtain a complete solution for the local electromagnetic field and to trace the observed modification to excitation of surface plasmons, localized plasmons in surface protrusions, shape (lightening rod) effects and surface polarization (image) effects. However, most experimental situations do not correspond to such simple geometries. For a distribution of (electromagnetically interacting) dielectric particles in another dielectric medium and more so

0039-6028/83/0000–0000/$03.00

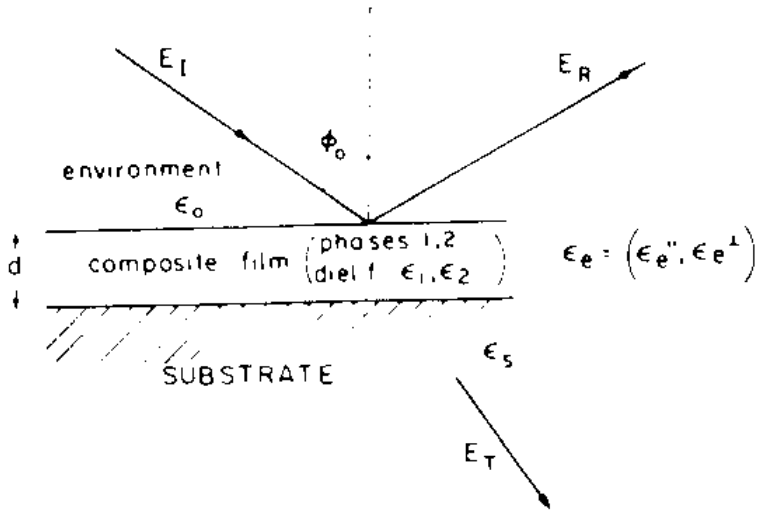

Fig. 1. A schematic description of a light scattering process involving a composite uniaxial film.

for a completely random mixture of two dielectric phases, a statistical approach is necessary.

Consider the model depicted in fig. 1. A substrate S (with dielectric function ε_S) is covered by a composite film (made of phases, 1, 2, ... with dielectric functions $\varepsilon_1, \varepsilon_2, \ldots$) in an environment characterized by a dielectric function ε_0. Note that usually one of the phases in the composite is identical to the environment 0. With the composite film we usually associate an effective dielectric function ε_e which is typically a uniaxial tensor with different parallel $\varepsilon_e^{\parallel}$ and perpendicular $\varepsilon_e^{\perp}$ components. Given ε_0, ε_e, ε_S and the film thickness d, it is possible to evaluate the transmission ($T = |E_T/E_I|^2$) and reflection ($R = |E_R/E_I|^2$) coefficients as well as phase and polarization properties of the transmitted and reflected light for any given incident beam. Alternatively by monitoring the reflected beam it is possible to obtain film information ($\varepsilon_e^{\parallel}$, $\varepsilon_e^{\perp}$ and film thickness d), which is the standard problem of ellipsometry [5]. Finally given some microscopic information about the film (e.g., the dielectric functions $\varepsilon_1, \varepsilon_2, \ldots$ and the volume fractions $P_1, P_2, \ldots$ of the pure phases) one can approximately calculate ε_e using one of several available approximations, the simplest of which is the Maxwell–Garnett method [6].

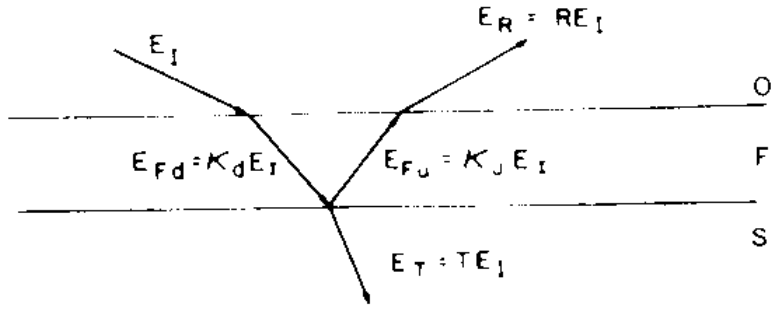

Fig. 2. A schematic description of a light scattering process involving a thin film. The coefficients R (reflection), T (transmission), κ_u and κ_d relate the various field amplitudes to the incident field.

It should be noted that the (elastic) light scattering experiments described above probe surface properties by monitoring the electromagnetic field far from the surface, and the results are interpreted in terms of a single film property – the effective dielectric tensor ε_e. There is no direct information about the electromagnetic field inside the film, though of course the average field $\langle E_F \rangle$ in the film can be easily found from Fresnel equations given ε_0, ε_e, ε_S and E_T.

When inelastic light scattering or resonance optical processes are considered we are usually concerned with the response of the molecules to the local EM field at the position of the molecule. Thus if the molecules are distributed homogeneously in phase 1 of the composite film, different optical processes associated with these molecules probe different moments $\langle |E_F|^n \rangle_1$ of the electric field in the film (the index 1 denotes averaging over the volume of phase 1). For absorption $n = 2$ while for higher order optical processes $n > 2$.

It is therefore of interest to consider higher order moments of the field intensity in composite materials. In two recent studies Bergman and Nitzan [7] and Aspnes [8] have considered the second moment $\langle |E|^2 \rangle$ for an infinite three-dimensional two-phase composite within the electrostatic approximation. In this problem the composite is taken to fill the volume between two (infinitely distant) plates of a capacitor [9] and a field E_0 is applied between these plates. E_0 is thus identical to the average field $\langle E(r) \rangle$ in the composite. A simple calculation leads to the remarkably simple result [7]

$$R_1 \equiv \frac{\langle |E(r)|^2 \rangle_1}{|E_0|^2} = \frac{1}{P_1} \frac{\mathrm{Im}(\varepsilon_e/\varepsilon_2)}{\mathrm{Im}(\varepsilon_1/\varepsilon_2)}, \tag{1.1}$$

which may be used to calculate the "enhancement ratio" R_1 given the pure $(\varepsilon_1, \varepsilon_2)$ and the effective (ε_e) dielectric functions are the volume fraction P_1.

When the composite under study constitutes a thin film on a given substrate the situation is considerably different. Instead of $E_0 = \langle E(r) \rangle$ we now have to distinguish between the incident field E_I and the average field in the film $\langle E_F(r) \rangle$. Also the EM field in the film is sensitive to the boundary conditions in the direction of finite thickness, and the geometry of a 3D system between the plates of a capacitor can no longer be used in the 2D case.

In this paper we provide an approximate solution for the intensity enhancement ratio

$$R_l = \frac{\langle |E_F|^2 \rangle_l}{|E_I|^2}, \quad l = 1, 2, \tag{1.2}$$

for a binary film in the model depicted in fig. 1. R_l is expressed as a function of ε_0, ε_1, ε_2, ε_S, d, the direction Φ_I of the incident radiation and of the incident polarization. The dependence on ε_1 and ε_2 enters through the film effective dielectric function ε_e which, together with the film thickness d, may be deduced

from ellipsometry measurements. Alternatively ε_e may be expressed as a function of ε_1, ε_2 and film composition and topography using one of the available theoretical methods [11–13]. A numerical study of a similar problem for a surface distribution of polarizable dipoles was recently carried out by Laor and Schatz [14].

As noted above the enhancement ratio (1.2) is useful for situations where the molecules of interest are distributed homogeneously in phase 1. A common alternative situation is one where the molecules of interest form a thin coating around the dielectric islands. It is therefore useful to estimate the enhancement ratio

$$R_{\text{shell}} = \frac{\langle |E_F|^2 \rangle_{\text{shell}}}{|E_1|^2}, \tag{1.3}$$

defined for a volume made of shells of a given thickness around each dielectric particle. In what follows we also calculate an approximation to this quantity.

The paper is organized as follows. In the next section we review the theory of light scattering from unisotropic thin films and use it to derive approximate expressions for the enhancement ratios defined above. In section 3 we review (and modify) available microscopic theories for the dielectric response of composite films and provide a framework for calculating the enhancement ratios R_1 and R_{shell} given the microscopic film structure. Results of numerical model calculations are given in section 4 and our conclusions are presented in section 5.

2. Evaluation of enhancement ratios

Our model is described in fig. 1 and consists of a substrate, a film and an environment with dielectric tensors ε_S, ε_e and ε_0 respectively. The magnetic permeability μ is taken to be 1 for all phases, ε_S and ε_0 are isotropic while ε_e is a uniaxial tensor with the optical axis perpendicular to the film surface. It is therefore characterized by two components, parallel $\varepsilon_e^{\parallel}$ and perpendicular $\varepsilon_e^{\perp}$. The film is composed of two phases, denoted by $l = 1, 2$. For this model we want to evaluate the intensity enhancement ratio

$$R_l = \langle |E_F|^2 \rangle_l / |E_1|^2, \quad l = 1, 2, \tag{2.1}$$

where E_1 is the incident field, E_F is the field in the film and where the index l ($l = 1, 2$) denotes average over the volume of the phase. We rewrite eq. (2.1) in the form

$$R_l = \frac{\langle |E_F^{\parallel}|^2 \rangle_l + \langle |E_F^{\perp}|^2 \rangle_l}{|E_1|^2} = R_l^{\parallel} \rho_{\parallel} + R_l^{\perp} \rho_{\perp}, \tag{2.2}$$

where

$$R_I^\delta = \langle |E_F^\delta|^2 \rangle_I / |\langle E_F^\delta \rangle|^2, \quad \delta = \|, \perp , \tag{2.3}$$

$$\rho_\delta = |\langle E_F^\delta \rangle|^2 / |E_I|^2, \quad \delta = \|, \perp . \tag{2.4}$$

$\langle E_F \rangle$ (with its normal and parallel components $\langle E_F^\delta \rangle$) is the field that would exist in a homogeneous film with a dielectric tensor ε_e. The calculation of R_I is now separated into the calculations at R_I^δ and of ρ_δ.

The factor ρ_δ may be extracted from the formalism which yields reflection and transmission coefficients associated with a uniaxial film of dielectric tensor ε_e with the symmetry axis perpendicular to the film surface [15]. The procedure is outlined in the appendix and the notation is defined in fig. 2. The results are:

s polarization (electric field E perpendicular to scattering plane)

$$\rho_\perp = 0, \tag{2.5a}$$

$$\rho_\| = |\kappa_d|^2 \exp(-\beta_2)\, |1 + r_{FS} \exp(i\beta)|^2, \tag{2.5b}$$

p polarization (electric field E in the scattering plane)

$$\rho_\perp = |\kappa_d|^2 \exp(-\beta_2)\, |1 + r_{FS} \exp(i\beta)|^2 |\sin \chi|^2, \tag{2.6a}$$

$$\rho_\| = |\kappa_d|^2 \exp(-\beta_2)\, |1 - r_{FS} \exp(i\beta)|^2 |\cos \chi|^2, \tag{2.6b}$$

where χ is the (complex) angle between the ray vector (direction of $\boldsymbol{E} \times \boldsymbol{H}$) in the film and the optical axis (the angle between $\langle \boldsymbol{E}_F \rangle$, the field in the effective homogeneous film, and the optical axis is $\pi - \chi$), κ_d is the (complex) coefficient relating the electric field amplitude of the "downgoing" (see fig. 2) wave in the film to the amplitude E_I of the incident field at the 0F interface and r_{FS} is the Fresnel reflection coefficient for a beam incident from F on the FS interface. Finally β and β_2 are defined by

$$\beta = (\omega d/c)\, N_F(\varphi_F) \cos(\varphi_F) = \beta_1 + i\beta_2, \tag{2.7}$$

where ω is the radiation frequency, c is the speed of light, d the film thickness, φ_F the (complex) angle between the wave vector $\boldsymbol{k}$ in the film and the optical axis and N_F is the (complex) refraction index in the film (which depends on φ_F for the p polarization case in a uniaxial medium). Explicit expressions for κ_d, χ, N_F and r_{FS} are given in the appendix. We note that these parameters are in general different for the s and p polarization cases. It should be kept in mind that for absorbing films the amplitude of the average field depends on the normal coordinate z (measured from the 0F interface. The expressions (2.5) and (2.6) for ρ were obtained taking $z = d/2$.

Turning now to the calculation of R_I^δ defined in eq. (2.3) we note that for an infinite three-dimensional isotropic binary composite this calculation is particularly simple. The starting point is the following definition of the effective dielectric function:

$$\varepsilon_e |\langle E \rangle|^2 = \varepsilon_1 P_1 \langle |E|^2 \rangle_1 + \varepsilon_2 P_2 \langle |E|^2 \rangle_2 , \tag{2.8}$$

in which ϵ_l and P_l are the dielectric function and the volume fraction of phase l and $\langle\ \rangle_l$ denotes an average over the volume of this phase (i.e. $\langle\ \rangle_l = (1/V_l)\int_l d\upsilon$). Dividing eq. (2.8) by ϵ_2 and taking its imaginary part leads directly to (1.1).

Generalization of (1.1) to a uniaxial medium is also simple. We assume that the two components are themselves isotropic so that the unisotropy of the composite results from its geometrical structure (i.e. parallel spheroides of one component immersed in the bulk of the other). Then eq. (2.8) is replaced by

$$\sum_{\delta} \epsilon_e^{\delta} |\langle E^{\delta}\rangle|^2 = \epsilon_1 P_1 \langle |E|^2\rangle_1 + \epsilon_2 P_2 \langle |E|^2\rangle_2, \tag{2.9}$$

where $\delta = \|, \perp$ denote directions with respect to a plane perpendicular to the optical axis. Define

$$R_1^{\delta} = \frac{1}{P_1} \operatorname{Im}(\epsilon_e^{\delta}/\epsilon_2)/\operatorname{Im}(\epsilon_1/\epsilon_2), \tag{2.10a}$$

$$R_2^{\delta} = \frac{1}{P_2} \operatorname{Im}(\epsilon_e^{\delta}/\epsilon_1)/\operatorname{Im}(\epsilon_2/\epsilon_1). \tag{2.10b}$$

The overall enhancement ratio for this case (uniaxial bulk) is then

$$\begin{aligned} R_1 &\equiv \langle |E|^2\rangle_1 / |\langle E\rangle|^2 = \left(\langle |E^{\|}|^2\rangle_1 + \langle |E^{\perp}|^2\rangle_1\right)/|\langle E\rangle|^2 \\ &= R_1^{\|} |\langle E^{\|}\rangle|^2/|\langle E\rangle|^2 + R_1^{\perp} |\langle E^{\perp}\rangle|^2/|\langle E\rangle|^2. \end{aligned} \tag{2.11}$$

An examination of electromagnetic wave propagation in a uniaxial medium (see appendix) shows that for a beam which is s-polarized relative to a plane normal to the optical axis $E^{\perp} = 0$, while for a p-polarized beam

$$|\langle E^{\|}\rangle/\langle E\rangle|^2 = |\cos\chi|^2, \quad |\langle E^{\perp}\rangle/\langle E\rangle|^2 = |\sin\chi|^2. \tag{2.12}$$

Thus

$$R_1 = \begin{cases} R_1^{\|}, & \text{s polarization} \\ R_1^{\|}|\cos\chi|^2 + R_1^{\perp}|\sin\chi|^2, & \text{p polarization} \end{cases} \tag{2.13}$$

If we adopt (2.9) as the definition of ϵ_e also for a film of finite thickness we can use the same procedure as above to obtain eqs. (2.10) with E_F^{δ} replacing E^{δ} everywhere) for the factors R_l^{δ} needed in eq. (2.2). The problem encountered at this point is the questionable validity of eqs. (2.8) or (2.9) for thin films. For an infinite three-dimensional composite, eq. (2.9) can be shown to be equivalent to the more conventional definition

$$\epsilon_e^{\delta}\langle E^{\delta}\rangle = \epsilon_1 P_1 \langle E^{\delta}\rangle_1 + \epsilon_2 P_2 \langle E^{\delta}\rangle_2. \tag{2.14}$$

The proof is based on the validity of the identity

$$\langle \epsilon |E|^2\rangle = \langle \epsilon E\rangle\langle E^*\rangle, \tag{2.15}$$

which may be shown [10] to hold under DC ($\omega = 0$) conditions in any three-dimensional medium with fixed potentials at the upper and lower boundaries (direction of the average field) and fixed normal derivatives of the potential at the other boundaries. For an infinite three-dimensional medium, and provided that the wavelength of the EM field is much larger than the length scale characterizing the inhomogeneous structure of the composite, (2.15) is valid because we can always impose the desired boundary conditions at infinity without affecting the field distribution in the bulk of the system. For a thin film the use of (2.15) is questionable and so is the equivalence of (2.14) and (2.9). Such equivalence can be established only if we assume that we can replace (at any given time) the potential at the lower and upper boundaries of the film by fixed potentials (on a length scale small relative to the wavelength; equal, say, to the average potentials on these boundaries) without affecting strongly the internal field distribution in the film.

Although this is a rather drastic assumption we have adopted eq. (2.2) with (2.5) and (2.6) and with (2.10) for R_l^δ, for estimating the intensity enhancement ratios in the film. Some justification to this may be given by noticing that also the use of the boundary conditions which lead to the Fresnel equations for the composite film actually involves a similar kind of assumption (namely the existence of a well defined boundary with the EM field amplitude depending only on the normal distance from this boundary).

The calculation described above is relevant if the molecules of interest are distributed homogeneously in the volume of phase l (because R_l, eq. (2.2), is the intensity enhancement averaged over the full volume of phase l). A more common situation for molecules adsorbed on island films is where the molecules occupy a thin shell covering each island (see fig. 3b below). It is possible also to estimate the intensity enhancement within such a volume. Consider for simplicity an island film made of spheres of dielectric function ϵ_2 in an environment of dielectric function ϵ_1 (fig. 3b), where the spheres are distributed in an ordered 2D lattice with one sphere per unit cell. We want the estimate

$$R_{\text{shell}} = \langle |E_F|^2 \rangle_{\text{shell}} / |E_I|^2, \tag{2.16}$$

where $\langle\ \rangle_{\text{shell}}$ denotes an average over the volume of a shell of thickness w around each sphere. Eq. (2.16) may be rewritten in the form

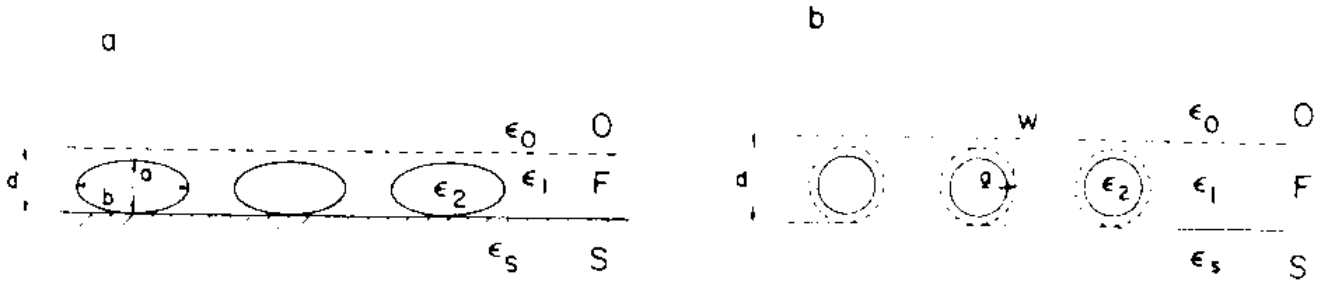

Fig. 3. Microscopic models of composite thin films used in the calculation of section 3.

$$R_{\text{shell}} = R^{\parallel}_{\text{shell}} + R^{\perp}_{\text{shell}}, \tag{2.17}$$

$$R^{\delta}_{\text{shell}} = R^{\delta}_{2}\rho_{\delta}S^{\delta}_{2}, \quad \delta = \parallel, \perp, \tag{2.18}$$

$$S^{\delta}_{2} = \langle |E^{\delta}_{\text{F}}|^2 \rangle_{\text{shell}} / \langle |E^{\delta}_{\text{F}}|^2 \rangle_{2}. \tag{2.19}$$

$\langle |E^{\delta}_{\text{F}}|^2 \rangle_2$ is the field averaged over the volume of the spheres or, under our assumptions, averaged over the volume of any single sphere. If we assume that the field is actually constant over such a volume (a similar assumption is made in the calculation of ε_e, see section 3) it can be shown that [16,17]

$$S^{\delta}_{2} = \frac{1}{9}\left[\left|\frac{\varepsilon_2}{\varepsilon_1} + 2\right|^2 + 2\left(\frac{a/2}{a/2 + w}\right)^3 \left|\frac{\varepsilon_2}{\varepsilon_1} - 1\right|^2\right], \tag{2.20}$$

where a is the sphere diameter. An equivalent result can be derived for ellipsoids. With R^{δ}_{2} and ρ_{δ} evaluated above, eqs. (2.15), (2.16) and (2.18) yield the desired estimate.

As seen above, the input to the desired calculation involves the film thickness d and the film effective dielectric tensor $\boldsymbol{\varepsilon}_e$ which may be obtained experimentally by ellipsometric methods. Alternatively we may use a microscopic model for the film and calculate $\boldsymbol{\varepsilon}_e$ from this model. This approach is reviewed in the next section.

3. A microscopic model for $\boldsymbol{\varepsilon}_e$

In this section we briefly review with some modifications the procedures used by Yamaguchi, Yoshida and Kinbara [11] and by Dignam and Moskovits [12] for calculating the effective dielectric properties of composite films. Even though the work of Dignam and Moskovits deals with molecular films while that of Yamaguchi et al. deals with metal island films, the mathematical treatment is similar because both calculations consider only dipolar interactions between the particles (molecules or islands). We follow Yamaguchi et al. [11] by considering the film to be made of a two-dimensional distribution of isolated islands, each has the shape of a spheroid of revolution with the symmetry axis perpendicular to the substrate plane (fig. 3). In what follows we shall consider the common situation where $\varepsilon_1 = \varepsilon_0$. An island j is characterized by the polarizabilities $\alpha^{\parallel}_j$ and $\alpha^{\perp}_j$ in the directions parallel and perpendicular to the surface. These polarizabilities include image effects such that the (point) dipole associated with a given island is taken to include the image of that island in the substrate. Thus

$$\alpha^{\perp}_j = \left(\alpha^{\perp}_j\right)^0 \left(1 - \frac{2\left(\alpha^{\perp}_j\right)^0}{a^3}\frac{\varepsilon_S - \varepsilon_0}{\varepsilon_S + \varepsilon_0}\right)^{-1} \frac{2\varepsilon_S}{\varepsilon_S + \varepsilon_0}, \tag{3.1a}$$

$$\alpha_j^{\parallel} = \left(\alpha_j^{\parallel}\right)^0 \left(1 - \frac{\left(\alpha_j^{\parallel}\right)^0}{a^3} \frac{\varepsilon_S - \varepsilon_0}{\varepsilon_S + \varepsilon_0}\right)^{-1} \frac{2\varepsilon_0}{\varepsilon_S + \varepsilon_0}, \tag{3.1b}$$

where $(\alpha_j^{\perp})^0$ and $(\alpha_j^{\parallel})^0$ are the "bare" polarizabilities associated with an isolated island and where a is the distance between the dipole and its image. For an isolated spheroid with a symmetry axis a and a perpendicular axis b, of dielectric function ε_2 in an environment with dielectric function ε_0, the bare polarizabilities are

$$\left(\alpha_j^{\delta}\right)^0 = \frac{1}{4\pi} \frac{\varepsilon_0}{L_\delta + \varepsilon_0/(\varepsilon_2 - \varepsilon_0)}, \quad 0 < L_\delta < 1, \quad L_\perp + 2L_\parallel = 1, \tag{3.2a}$$

where

$$L_\perp = \begin{cases} \dfrac{1}{\eta^2 - 1}\left(\dfrac{\eta}{(\eta^2 - 1)^{1/2}} \cosh^{-1}\eta - 1\right), & \text{prolate, } a > b, \\ \dfrac{1}{1 - \eta^2}\left(1 - \dfrac{\eta}{(1 - \eta^2)^{1/2}} \cos^{-1}\eta\right), & \text{oblate, } a < b \end{cases} \tag{3.2b}$$

$$L_\parallel = \tfrac{1}{2}(1 - L_\perp). \tag{3.2c}$$

Of the factors multiplying $(\alpha_j^{\delta})^0$ in eqs. (3.1) one arizes from the field induced on the dipole by its own image and the other from summing the contributions to the dipole induced at site j from the actual dipole and from its image. Note that the distance between the dipole and its image is taken to be equal to a, the symmetry axis of the spheroid.

Other parameters associated with the film are n, the number of islands per unit area, and d, the film thickness. The thickness d is well defined only for films with thickness much larger than the characteristic inhomogeneous length (e.g. particle size) and, for the film of fig. 3, is to a large extent arbitrary.

In the treatments of Yamaguchi et al. [11] and of Dignam and Moskovits [12] the islands are assumed to be well separated from each other so that their electromagnetic interactions may be approximated as interactions between point dipoles. The effective dielectric tensor of the film is calculated in the following way: First the point dipoles $\boldsymbol{\mu}_j$ associated with the islands are calculated by solving the system of coupled equations

$$\boldsymbol{\mu}_j = \boldsymbol{\alpha}_j \left(\boldsymbol{E}_0(\boldsymbol{r}_j) + \sum_{\substack{k \\ k \neq j}} \boldsymbol{E}_{jk}\right), \tag{3.3}$$

where $\boldsymbol{E}_0(\boldsymbol{r}_j)$ is the field that will be at the point $\boldsymbol{r}_j$ in the absence of the film (in general this is different from the incident field because of the presence of the substrate) and where $\boldsymbol{E}_{jk}$ is the field induced at the point j by the dipole

occupying the point k. (In the electrostatic limit E_0 is constant and $\boldsymbol{E}_{jk}$ is given by

$$\boldsymbol{E}_{jk} = \frac{3\hat{n}_{jk}(\boldsymbol{\mu}_k \cdot \hat{n}_{jk}) - \boldsymbol{\mu}_k}{\varepsilon_0 |r_{jk}|^3}, \tag{3.4}$$

where $|r_{jk}| = |\boldsymbol{r}_j - \boldsymbol{r}_k|$ and where $\hat{n}_{jk} = \boldsymbol{r}_{jk}/|r_{jk}|$). Secondly the contribution P of the induced dipoles to the polarization is calculated from

$$\boldsymbol{P} = \frac{n}{Nd} \sum_{j=1}^{N} \boldsymbol{\mu}_j. \tag{3.5}$$

Finally the effective dielectric functions $\varepsilon_e^{\parallel}$ and $\varepsilon_e^{\perp}$ are obtained from

$$\frac{\varepsilon_e^{\delta} - \varepsilon_1}{4\pi} \langle E_F^{\delta} \rangle = P^{\delta}, \tag{3.6}$$

where $\langle E_F^{\parallel} \rangle$ and $\langle E_F^{\perp} \rangle$ are the components of the average field in the film.

Using this procedure in the electrostatic limit, Dignam and Moskovits [12] obtain (their results are generalized below to the case $\varepsilon_0 \neq 1$)

$$\varepsilon_e^{\delta} = \varepsilon_0 + \varepsilon_0 \frac{E_0^{\delta}}{\langle E_F^{\delta} \rangle} \frac{\gamma_{\delta}}{d}, \tag{3.7}$$

where

$$\gamma_{\delta} = \frac{4\pi n}{\varepsilon_0 E_0^{\delta}} \langle \mu^{\delta} \rangle. \tag{3.8}$$

Here $\langle \mu^{\delta} \rangle$ is the average dipole ($= N^{-1} \sum_{j=1}^{N} \mu_j^{\delta}$). It is given by [18]

$$\langle \mu^{\delta} \rangle \frac{\langle \alpha^{\delta} \rangle E_0^{\delta}}{1 - \langle \alpha^{\delta} \rangle \theta_{\delta} \langle f^{\delta} \rangle} g^{\delta}, \tag{3.9a}$$

$$g^{\perp} = \left[2\varepsilon_S/(\varepsilon_S + \varepsilon_0)\right]^{-1}, \quad g^{\parallel} = \left[2\varepsilon_0/(\varepsilon_S + \varepsilon_0)\right]^{-1}, \tag{3.9b}$$

in which α^{δ} is the average island polarizability ($N^{-1} \sum_{j=1}^{N} \alpha_j$) in the parallel ($\delta = \parallel$) and perpendicular ($\delta = \perp$) directions and θ_{δ} is given by

$$\theta_{\delta} = \langle \mu^{\delta} f^{\delta} \rangle / \langle \mu^{\delta} \rangle \langle f^{\delta} \rangle. \tag{3.10}$$

in eqs. (3.9) and (3.10) f_j^{δ} is the sum of dipole interaction terms,

$$f_j^{\delta} = \sum_{\substack{k \\ k \neq j}} F_{jk}^{\delta}, \quad \delta = x, y, z, \tag{3.11}$$

where x–y is the film plane and x_{jk}, y_{jk} are the components of the distance between the j and k dipoles,

$$F_{jk}^{x} = \frac{2x_{jk}^2 - y_{jk}^2}{\varepsilon_0 \left(x_{jk}^2 + y_{jk}^2\right)^{5/2}}, \tag{3.12a}$$

$$F_{jk}^{y} = \frac{2y_{jk}^2 - x_{jk}^2}{\varepsilon_0\left(x_{jk}^2 + y_{jk}^2\right)^{5/2}}, \tag{3.12b}$$

$$F_{jk}^{z} = -\frac{1}{\varepsilon\left(x_{jk}^2 + y_{jk}^2\right)^{3/2}}. \tag{3.12c}$$

Taking the configurational average we have

$$\langle f^x \rangle = \langle f^y \rangle = \langle f^{\parallel} \rangle = f, \tag{3.13a}$$

$$\langle f^z \rangle = \langle f^{\perp} \rangle = -2f, \tag{3.13b}$$

where

$$f = \frac{1}{2\varepsilon_0}\Big\langle \sum_{\substack{k \\ k \neq j}} \left(x_{jk}^2 + y_{jk}^2\right)^{-3/2} \Big\rangle \tag{3.14}$$

may be computed numerically for any given configuration. It should be noted that the above results are obtained using the assumption that α_j is not correlated with $\sum_{k \neq j} F_{jk}\mu_k$.

The appearance of θ (eq. (3.10)) in the expression for ε_e (eqs. (3.1)–(3.9)) makes the calculation difficult in general. However in some cases θ becomes constant [11]:

(a) If the islands are distributed in an ordered lattice with one island per unit cell then $\sum_{k \neq j} F_{jk}$ is independent of the site j and $\theta = 1$.

(b) If the density n of particles is high so that there are many particles contributing over a range where F_{jk} changes little. $\sum_{k \neq j} F_{jk}$ will depend only weakly on j and $\theta \sim 1$.

(c) If the density n of particles is very low μ_j depends only weakly on the position of the dipole j and again $\theta \sim 1$.

In the calculations reported below we have assumed that conditions for taking $\theta = 1$ are satisfied. We note that in such cases a resonance in the island polarizability implies a resonance behaviour of ε_e (e.g. the so-called "conduction electron resonances"). This is seen in (3.9) written in the form

$$\langle \mu^{\delta} \rangle = \left[\langle \alpha^{\delta} \rangle^{-1} - \theta_{\delta}\langle f^{\delta} \rangle\right]^{-1} E_0^{\delta} g^{\delta}.$$

The term $\theta_{\delta}\langle f^{\delta} \rangle$ is seen to yield shift and broadening of the bare (single island) resonance. Additional broadening is obtained if $\langle \alpha^{\delta} \rangle$ is related to a distribution of particle shapes with different resonance frequencies associated with different shapes. It should be kept in mind that if conditions for θ = constant are not met, an important source of broadening is the different resonance behaviour associated with different local structures (clusters of islands). Eqs. (3.7)–(3.10) with $\theta = 1$ cannot account for this effect which is seen, e.g., in a full numerical solution of eq. (3.3) [14].

Returning to eq. (3.6) we note that in order to make it into an equation for ε_e, the ratio $E_0^\delta/\langle E_F^\delta\rangle$ between the field E_0^δ that would be there in the absence of the film and the average field $\langle E_F^\delta\rangle$ in the film, has to be expressed as a function of ε_e^δ. Yamaguchi et al. [11] as well as Dignam and Moskovits [12] use

$$E_0^{\parallel}/\langle E_F^{\parallel}\rangle = 1, \tag{3.15a}$$

$$E_0^{\perp}/\langle E_F^{\perp}\rangle = \varepsilon_e/\varepsilon_0, \tag{3.15b}$$

This ansatz is equivalent to the assumption that E_0 is identical to E_I, the incident field. In fact, E_0 is different from E_I due to the presence of a reflected field. For s polarization

$$E_0^{\parallel} = (1 + r_{0S})E_I, \tag{3.16}$$

while for p polarization

$$E_0^{\parallel} = (1 - r_{0S})E_I \cos\varphi_0, \tag{3.17a}$$

$$E_0^{\perp} = (1 + r_{0S})E_I \sin\varphi_0. \tag{3.17b}$$

$\langle E_F^\delta\rangle$ may be obtained using the same procedure that leads to the ρ factors of eqs. (2.5) and (2.6). For s polarization

$$\langle E_F^{\parallel}\rangle = \kappa_d\, e^{-\beta_2/2}\left(1 + r_{FS}\, e^{i\beta}\right)E_I \tag{3.18}$$

and for p polarization

$$\langle E_F^{\parallel}\rangle = \kappa_d\, e^{-\beta_2/2}\left(1 - r_{FS}\, e^{i\beta}\right)E_I \cos\chi, \tag{3.19a}$$

$$\langle E_F^{\perp}\rangle = \kappa_d\, e^{-\beta_2/2}\left(1 + r_{FS}\, e^{i\beta}\right)E_I \sin\chi, \tag{3.19b}$$

The parameters κ_d, β, β_2, r and χ are defined and given in terms of ε_e in section 2 and the appendix.. We note that the numerical values of these parameters are different in the s and p polarization cases. We note that $\langle E_F\rangle$, eqs. (3.18) and (3.19), was calculated as in section 2 in the middle of the film.

Eqs. (3.16)–(3.19) lead to

$$\frac{E_0^{\parallel}}{\langle E_F^{\parallel}\rangle} = \begin{cases} \dfrac{1 - r_{0S}}{\kappa_d\, e^{-\beta_2/2}\left(1 + r_{FS}\, e^{i\beta}\right)}, & \text{s polarization,} \\[2ex] \dfrac{(1 - r_{0S})\cos\varphi_0}{\kappa_d\, e^{-\beta_2/2}\left(1 - r_{FS}\, e^{i\beta}\right)\sin\chi}, & \text{p polarization,} \end{cases} \tag{3.20}$$

$$\frac{E_0^{\perp}}{\langle E_F^{\perp}\rangle} = \frac{(1 + r_{0S})\sin\varphi_0}{\kappa_d\, e^{-\beta_2/2}\left(1 + r_{FS}\, e^{i\beta}\right)\cos\chi}, \quad \text{p polarization,} \tag{3.21}$$

Eq. (3.7) with (3.20) or (3.21) may be used to solve iteratively for $\varepsilon_e^{\parallel}$ or $\varepsilon_e^{\perp}$. It should be noted however that since the ratio $E_0^\delta/\langle E_F^\delta\rangle$ calculated from eqs. (3.16)–(3.19) is in general a function of the polarization (s or p) and of the

incident angle, the resulting ε_e will depend on these experimental variables. In other words, this procedure leads to the conclusion that unlike in the infinite bulk situation, it is impossible in the thin *composite* film case to associate results of light scattering experiments with a single dielectric tensor ε_e. This observation suggests that ellipsometric measurements using varying angles should be carried out in order to elucidate the importance of this effect [19].

On the other hand, in many cases the degree of ambiguity in such determinations of ε_e is not large. With this in mind we have performed most of our calculations using eqs. (3.7) and (3.15), and checked for several cases the solution so obtained against the more rigorous approach based on eqs. (3.20) and (3.21).

Next we consider corrections to the electrostatic limit. We shall still assume that the particles are small enough so that retardation effects may be neglected over the size of a single island. However, if the characteristic distance between islands is not much smaller than the radiation wavelength, retardation effects cannot be disregarded in evaluating the inter-island interaction. To take this into account the field $\boldsymbol{E}_{jk}$ of eq. (3.3) is calculated from

$$\boldsymbol{E}_{jk} = \exp(\mathrm{i}|k|r_{jk})\left[\frac{|k|^2(\hat{n}_{jk}\times\boldsymbol{\mu}_k)\times\hat{n}_{jk}}{|r_{jk}|} + \left[3\hat{n}_{jk}(\hat{n}_{jk}\cdot\boldsymbol{\mu}_k)-\boldsymbol{\mu}_k\right]\left(\frac{1}{|r_{jk}|^3}-\frac{\mathrm{i}k}{|r_{jk}|^2}\right)\right], \tag{3.22}$$

where $|k| = 2\pi/\lambda_0$, and λ_0 is the incident wavelength. The rest of the calculation follows a route identical to that described above [20]. It should be kept in mind that the concept of a dielectric function is questionable when the distance between the islands is larger than the wavelength. We nevertheless follow Yamaguchi et al. [11] in carrying out such a calculation which can at least provide a feeling for the range of validity of the electrostatic approach.

4. Numerical results

Let us first summarize the results of sections 2 and 3 which are used in the calculations reported below. The intensity enhancement ratio for phase 1 (fig. 3a),

$$R_1 = \langle|E_F|^2\rangle/|E_I|^2, \tag{4.1}$$

is given by

$$R_1 = R_1^{\parallel}\rho_{\parallel} + R_1^{\perp}\rho_{\perp}, \tag{4.2}$$

with ($\delta = \|, \perp$)

$$\rho_\delta = |\langle E_F^\delta \rangle|^2 / |E_I|^2, \quad R_1^\delta = \langle |E_F^\delta|^2 \rangle / |\langle E_F^\delta \rangle|^2. \tag{4.3}$$

The ρ_δ factor is given by, for s polarization,

$$\rho_\perp = 0, \quad \rho_\| = |\kappa_d|^2 \exp(-\beta_2)\, |1 + r_{FS} \exp(i\beta)|^2, \tag{4.4}$$

and for p polarization

$$\rho_\perp = |\kappa_d|^2 \exp(-\beta_2)\, |1 + r_{FS} \exp(i\beta)|^2 |\sin\chi|^2, \tag{4.5a}$$

$$\rho_\| = |\kappa_d|^2 \exp(-\beta_2)\, |1 - r_{FS} \exp(i\beta)|^2 |\cos\chi|^2. \tag{4.5b}$$

The R_1^δ factor is given by

$$R_1^\delta = \frac{1}{P_1} \mathrm{Im}(\varepsilon_e^\delta / \varepsilon_2) / \mathrm{Im}(\varepsilon_1 / \varepsilon_2), \tag{4.6}$$

where ε_1 and ε_2 are the dielectric functions of the two components constituting the film, P_1 is the volume fraction of component 1 in the film and ε_e is the effective dielectric tensor of the film. The other parameters appearing in eqs. (4.4) and (4.5) are given in terms of ε_e, ε_0, the dielectric function of the environment, ε_S, the dielectric function of the substrate, and φ_0, the incident angle (between the incident $\boldsymbol{k}$ vector and the surface normal). These are

$$\sin^2\chi = \sin^2\varphi_F / \left[\sin^2\varphi_F + \left(\varepsilon_e^\perp / \varepsilon_e^\|\right) \cos^2\varphi_F\right], \tag{4.7}$$

$$\sin\varphi_F = \left(\sqrt{\varepsilon_0} / N_F(\varphi_F)\right) \sin\varphi_0, \tag{4.8}$$

$$N_F(\varphi_F) = \begin{cases} \sqrt{\varepsilon_e^\|}, & \text{s polarization,} \\ \left(\dfrac{\sin^2\varphi_F}{\varepsilon_e^\perp} + \dfrac{\cos^2\varphi_F}{\varepsilon_e^\|} \right)^{1/2}, & \text{p polarization,} \end{cases} \tag{4.9}$$

$$\beta = N_F(\varphi_F)\, (\omega d / c) \cos\varphi_F, \tag{4.10}$$

where ω is the radiation frequency, c the speed of light and d the film thickness,

$$\beta_2 = \mathrm{Im}(\beta), \tag{4.11}$$

$$\kappa_d = \frac{t_{0F}}{1 + r_{0F} r_{FS} \exp(2i\beta)}, \tag{4.12}$$

$$t_{0F} = \begin{cases} \dfrac{2\sqrt{\varepsilon_0}\, \cos\varphi_0}{\sqrt{\varepsilon_0}\, \cos\varphi_0 + N_F \cos\varphi_F}, & \text{s polarization,} \\ 2\left(\dfrac{\varepsilon_e^\perp \sin\chi}{\varepsilon_0 \sin\varphi_0} + \dfrac{\cos\chi}{\cos\varphi_0} \right)^{-1}, & \text{p polarization,} \end{cases} \tag{4.13}$$

$$r_{0F} = \begin{cases} \dfrac{\sqrt{\varepsilon_0}\cos\varphi_0 - N_F\cos\varphi_F}{\sqrt{\varepsilon_0}\cos\varphi_0 + N_F\cos\varphi_F}, & \text{s polarization,} \\ \left(\dfrac{\varepsilon_e^{\perp}\sin\chi}{\varepsilon_0\sin\varphi_0} - \dfrac{\cos\chi}{\cos\varphi_0}\right)\left(\dfrac{\varepsilon_e^{\perp}\sin\chi}{\varepsilon_0\sin\varphi_0} + \dfrac{\cos\chi}{\cos\varphi_0}\right)^{-1}, & \text{p polarization,} \end{cases} \tag{4.14}$$

$$r_{FS} = \begin{cases} \dfrac{N_F\cos\varphi_F - \sqrt{\varepsilon_S}\cos\varphi_S}{N_F\cos\varphi_F + \sqrt{\varepsilon_S}\cos\varphi_S}, & \text{s polarization,} \\ \left(\dfrac{\varepsilon_S\sin\varphi_S}{\varepsilon_e^{\perp}\sin x} - \dfrac{\cos\varphi_S}{\cos x}\right)\left(\dfrac{\varepsilon_S\sin\varphi_S}{\varepsilon_e^{\perp}\sin x} + \dfrac{\cos\varphi_S}{\cos x}\right)^{-1}, & \text{p polarization.} \end{cases} \tag{4.15}$$

In the film model of fig. 3a, ε_e is calculated in terms of ε_1, the island surface density n, the island polarizabilities $\alpha^{\parallel}$ and $\alpha^{\perp}$ and the lattice sums $f^{\perp}$ and $f^{\parallel}$ from

$$\varepsilon_e^{\delta} = \varepsilon_1\left(1 + \frac{4\pi n}{\varepsilon_1 d}\,\frac{\langle\alpha^{\delta}\rangle}{1 - \langle\alpha^{\delta}\rangle\langle f^{\delta}\rangle\theta_{\delta}}\right), \tag{4.16}$$

$$\langle f^{\parallel}\rangle = -\frac{1}{2}\langle f^{\perp}\rangle = \frac{1}{2\varepsilon_0}\Big\langle \sum_{\substack{k \\ k\neq j}} r_{jk}^{-3}\Big\rangle, \tag{4.17}$$

where r_{jk} is the distance between dipoles j and k,

$$\theta = \langle\mu^{\delta}f^{\delta}\rangle/\langle\mu^{\delta}\rangle\langle f^{\delta}\rangle. \tag{4.18}$$

The averages are over all islands. $\theta = 1$ for an ordered lattice of islands. For the ratio $E_0^{\delta}/\langle E_F^{\delta}\rangle$ we used either the ansatz [10,11]

$$E_0^{\parallel}/\langle E_F^{\parallel}\rangle = 1, \quad E_0^{\perp}/\langle E_F^{\perp}\rangle = \varepsilon_e^{\perp}/\varepsilon_0 \tag{4.19}$$

or the rigorous expressions

$$\frac{E_0^{\parallel}}{\langle E_F^{\parallel}\rangle} = \begin{cases} \dfrac{1 + r_{0S}}{\kappa_d\exp(-\beta_2/2)\,(1 + r_{FS}\exp(i\beta))}, & \text{s polarization,} \\ \dfrac{(1 - r_{0S})\cos\rho_0}{\kappa_d\exp(-\beta_2/2)\,(1 - r_{FS}\exp(i\beta))\sin\chi}, & \text{p polarization,} \end{cases} \tag{4.20}$$

$$\frac{E_0^{\perp}}{\langle E_F^{\perp}\rangle} = \frac{(1 + r_{0S})\sin\varphi_0}{\kappa_d\exp(-\beta_2/2)\,(1 + r_{FS}\exp(i\beta))\cos\chi}, \tag{4.21}$$

$$r_{0S} = \begin{cases} \dfrac{\sqrt{\varepsilon_0}\cos\varphi_0 - \sqrt{\varepsilon_S}\cos\varphi_S}{\sqrt{\varepsilon_0}\cos\varphi_0 + \sqrt{\varepsilon_S}\cos\varphi_S}, & \text{s polarization,} \\ \dfrac{\sqrt{\varepsilon_S}\cos\varphi_0 - \sqrt{\varepsilon_0}\cos\varphi_S}{\sqrt{\varepsilon_S}\cos\varphi_0 + \sqrt{\varepsilon_0}\cos\varphi_S}, & \text{p polarization.} \end{cases} \tag{4.22}$$

For islands of spheroidal shapes with symmetry axis perpendicular to the surface the island polarizabilities are

$$\alpha^{\perp} = \frac{2\varepsilon_S}{\varepsilon_S + \varepsilon_0}\frac{1}{4\pi}\frac{\varepsilon_0}{L_{\perp} + \varepsilon_0/(\varepsilon_2 - \varepsilon_0)}, \tag{4.23a}$$

$$\alpha^{\parallel} = \frac{2\varepsilon_0}{\varepsilon_S + \varepsilon_0}\frac{1}{4\pi}\frac{\varepsilon_0}{L_{\parallel} + \varepsilon_0/(\varepsilon_2 - \varepsilon_0)}, \tag{4.23b}$$

where $L_{\parallel}$ and $L_{\perp}$ are given by eq. (3.2b). Eqs. (4.1)–(4.23) were used to obtain most of the results reported below. In addition we have performed calculations using eq. (3.22) to assess the importance of retardation effects, and using eqs. (2.14)–(2.16) and (2.18) to obtain intensity enhancement ratios for spherical shells.

To calculate the island polarizabilities we have used the bulk dielectric function of silver, corrected for finite size effects in the following way [11]: Let $\varepsilon_2 = \varepsilon_2' + i\varepsilon_2''$ and take the typical size of an island to be A. Then the imaginary part is replaced by $\bar{\varepsilon}_2''$ given by [11,12]

$$\bar{\varepsilon}_2'' = \varepsilon_2''\left(1 + 8\omega_p/3A\omega_\tau\right), \tag{4.24}$$

where ω_p and ω_τ are the bulk plasma frequency and the bulk relaxation rate of the electrons. We follow Yamaguchi et al. [11] in taking the values for silver $\omega_p = 1.4 \times 10^{16}\ s^{-1}$ and $\omega_\tau = 0.0105\omega + 2.74 \times 10^{13}\ s^{-1}$.

In some of the calculations we have also taken into account radiation damping contributions to the island polarizability following the simplified approach of Wokaun, Gordon and Liao [21]. This is done by replacing the bare island polarizability $(\alpha_j^{\delta})^0$ of eqs. (3.1) by an effective polarizability which includes the effect of radiation damping,

$$\left(\alpha_j^{\delta}\right)^0 \to \left(\alpha_j^{\delta}\right)^0_{\text{eff}} = \frac{\left(\alpha_j^{\delta}\right)^0}{1 - i\left(\alpha_j^{\delta}\right)^0 16\pi^3 V_j/3\varepsilon_0\lambda_0^3}, \tag{4.25}$$

where λ_0 is the incident wavelength.

We now describe the results of some model calculations. Unless otherwise stated the substrate taken in these calculations is quartz ($\varepsilon_S = 2.13$) and the environment is vacuum or air ($\varepsilon_0 = \varepsilon_1 = 1.0$). Also the film thickness d is arbitrarily chosen to be $1.1a$, a being the particle size along its symmetry axis.

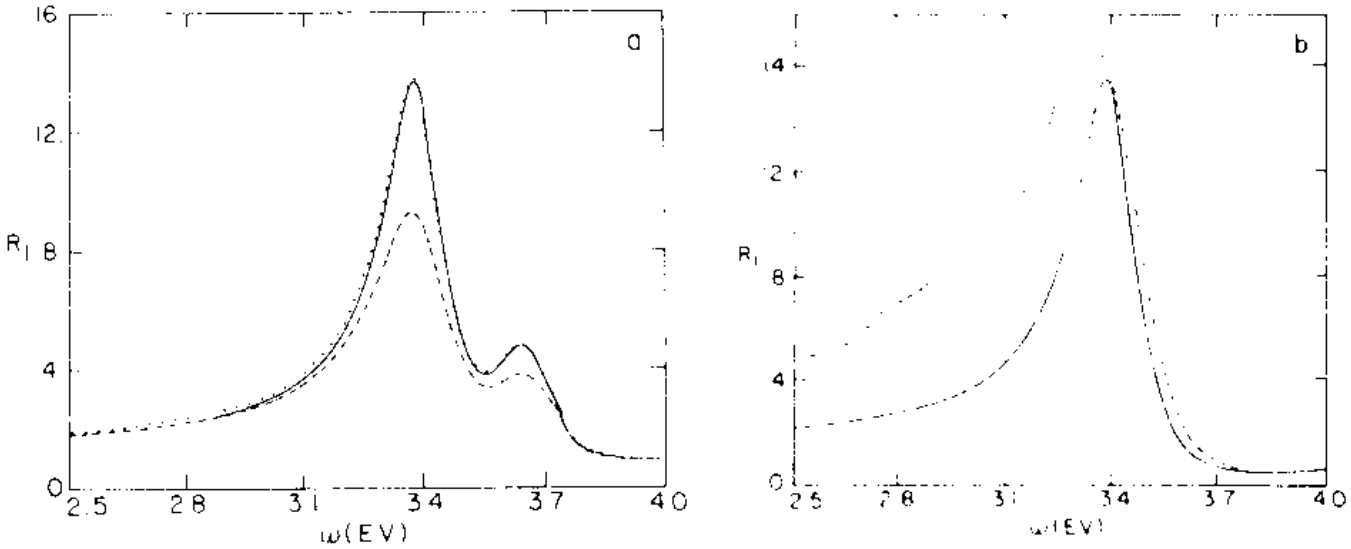

Fig. 4. Enhancement ratio R_1 as a function of incident light frequency for a film made of silver spheres (radius 100 Å) on quartz in vacuum. Sphere density is $n = 1.1 \times 10^{11}$ cm^{-2}. (a) Full line, calculation based on the electrostatic approximation using the bulk dielectric function of silver; dashed line, calculation taking into account finite size effect (eq. (4.24)) on the dielectric function; dotted line, calculation taking into account radiation damping (eq. (4.25)); $\varphi = 45°$. (b) Full line, calculation based on the electrostatic approximation using the bulk dielectric function of silver; dashed line, calculation taking retardation effects into account (eq. (3.22)) using the bulk dielectric function of silver; $\varphi = 0°$.

In fig. 4 we plot R_1 versus the radiation frequency ω for a film modeled by a square lattice of silver spheres. The sphere radius is 100 Å and the nn distance between centres (lattice constant) is 300 Å. In fig. 4a we compare the results obtained for a p-polarized radiation incident at $\varphi_0 = 45°$, where for ε_2 we use the bulk dielectric function of silver, corrected for finite size as well as for radiation damping (eqs.(4.24) and (4.25)). In fig. 4b we compare for the same model with $\varphi_0 = 0$ the results obtained from the electrostatic approximation and from a calculation which includes retardation in the sphere-sphere interaction. It is seen that for the parameter used these corrections have only a modest effect on the resulting intensity enhancement. Large effects are obtained in different ranges of the parameters as seen below.

In fig. 5 we compare the result obtained for an ordered square lattice and identical particles to that obtained for the same density of identical particles randomly distributed in the plane and also to the result for a square lattice of particles with a random shape distribution. In this calculation ε_2 was taken as the bulk dielectric function of silver. The particle density is $n = 1 \times 10^{-5}$ Å^{-2} and they are taken in this calculation to be prolate spheroids with $a = 200$ Å and $b = 100$ Å (or $\langle b \rangle = 100$ Å for the random case). The shape distribution is obtained by using the log-Gauss distribution for b,

$$P(b) = \frac{\exp\{-[\ln(b/\langle b \rangle)]^2/2\sigma^2\}}{\sqrt{2\pi}\,\sigma b}.$$

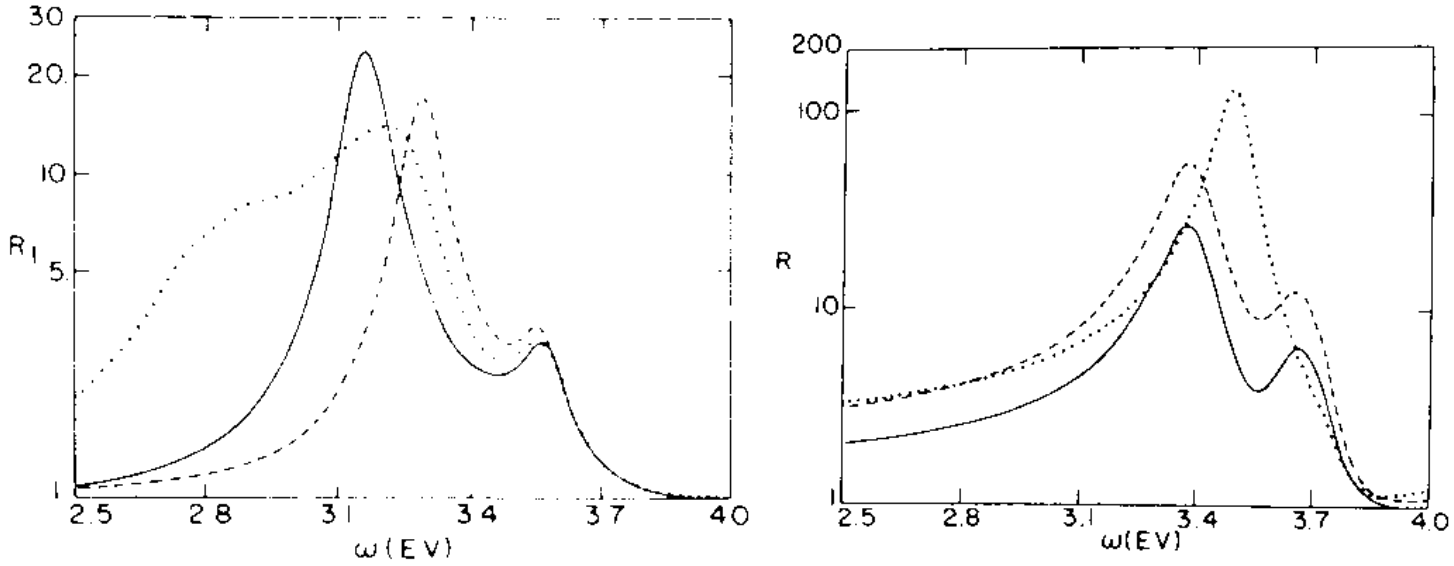

Fig. 5. Enhancement ratio R_1 as a function of incident light frequency using the bulk dielectric function of silver. The film is made of prolate spheroids with the axis normal to the plane. $a = 200$ Å, $n = 1.0 \times 10^{11}$ cm^{-2}, $\varphi = 45°$. Full line, ordered square lattice of spheroids with fixed shape, $\eta = a/b = 2.0$; dashed line, distribution of spheroids ($\eta = 2.0$) with random positions; dotted line, square array of spheroids of random shape (see text) with $\langle b \rangle = 100$ Å.

Fig. 6. Enhancement ratio as a function of incident light frequency in a film made of a square array of silver spheres (radius 50 Å; density 5×10^{11} cm^{-2}; $\varphi = 45°$; bulk dielectric function of silver) on quartz in vacuum. Full line, intensity averaged over the entire film volume outside the silver spheres; dashed line, intensity averaged over shells of thickness $w = 10$ Å around each sphere; dotted line, intensity averaged over a shell as above for an isolated silver sphere in vacuum.

We have taken $\sigma = 0.2$.

It is seen that positional randomness has a relatively small effect on the result while randomness in shape leads to a considerable broadening of the resonance behaviour. It should be noted again that our approximation (following Yamaguchi et al. [11] and Dignam and Moskovits [12]) cannot account for one important aspect of positional randomness (discussed in section 3) which may in some situations lead to large broadening.

In fig. 6 we compare the enhancement ratio R_1 associated with a square array of silver spheres (radius 50 Å; ε_2 taken to be the bulk dielectric function of silver; the sphere density is $n = 5 \times 10^{-5}$ Å^{-2}) to R_{shell} (eq. (2.14)), for a shell of thickness $w = 10$ Å around each sphere in the same array, and to R_{shell} calculated for an isolated sphere (using the expression

$$R_{\text{shell}} = 1 + \left(\frac{a/2}{a/2 + w} \right)^3 \left| \frac{\varepsilon_2 - \varepsilon_0}{\varepsilon_2 + \varepsilon_0} \right|^2 ,$$

or taking a very low density of spheres in the calculation based on eq. (2.14)). The difference (of about a factor 3 for the parameters used) between R_1, the enhancement average over the whole volume outside the spheres, and R_{shell} is

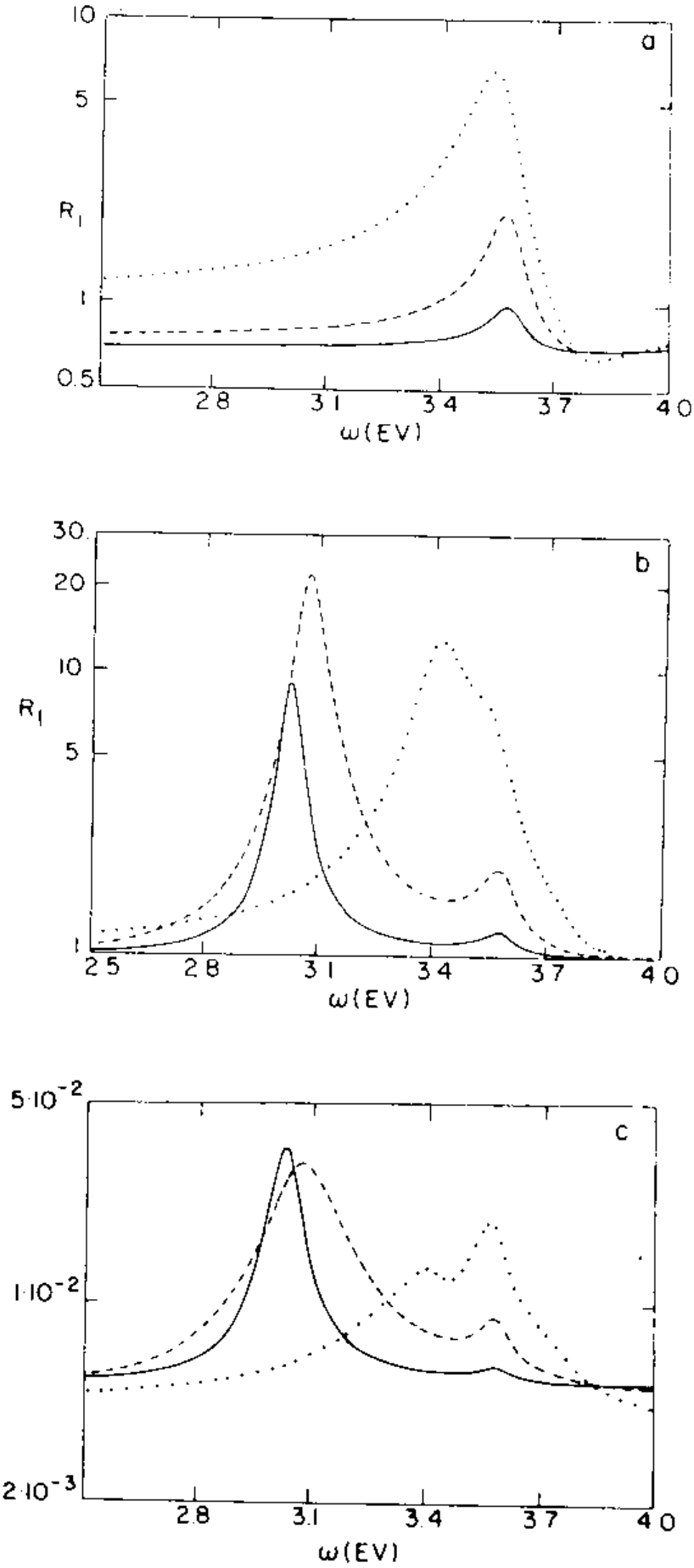

Fig. 7. Enhancement ratio R_1 as a function of incident frequency for a square array of prolate silver spheroids ($a = 200$ Å, $\eta = 2.0$, bulk dielectric function of silver) on quartz in vacuum. Full line, $n = 1 \times 10^{10}$ cm^{-2}, dashed line, $n = 5 \times 10^{10}$ cm^{-2}; dotted line, $n = 2.5 \times 10^{11}$ cm^{-2}. (a) $\varphi = 0°$; (b) $\varphi = 45°$; (c) $\varphi = 89°$.

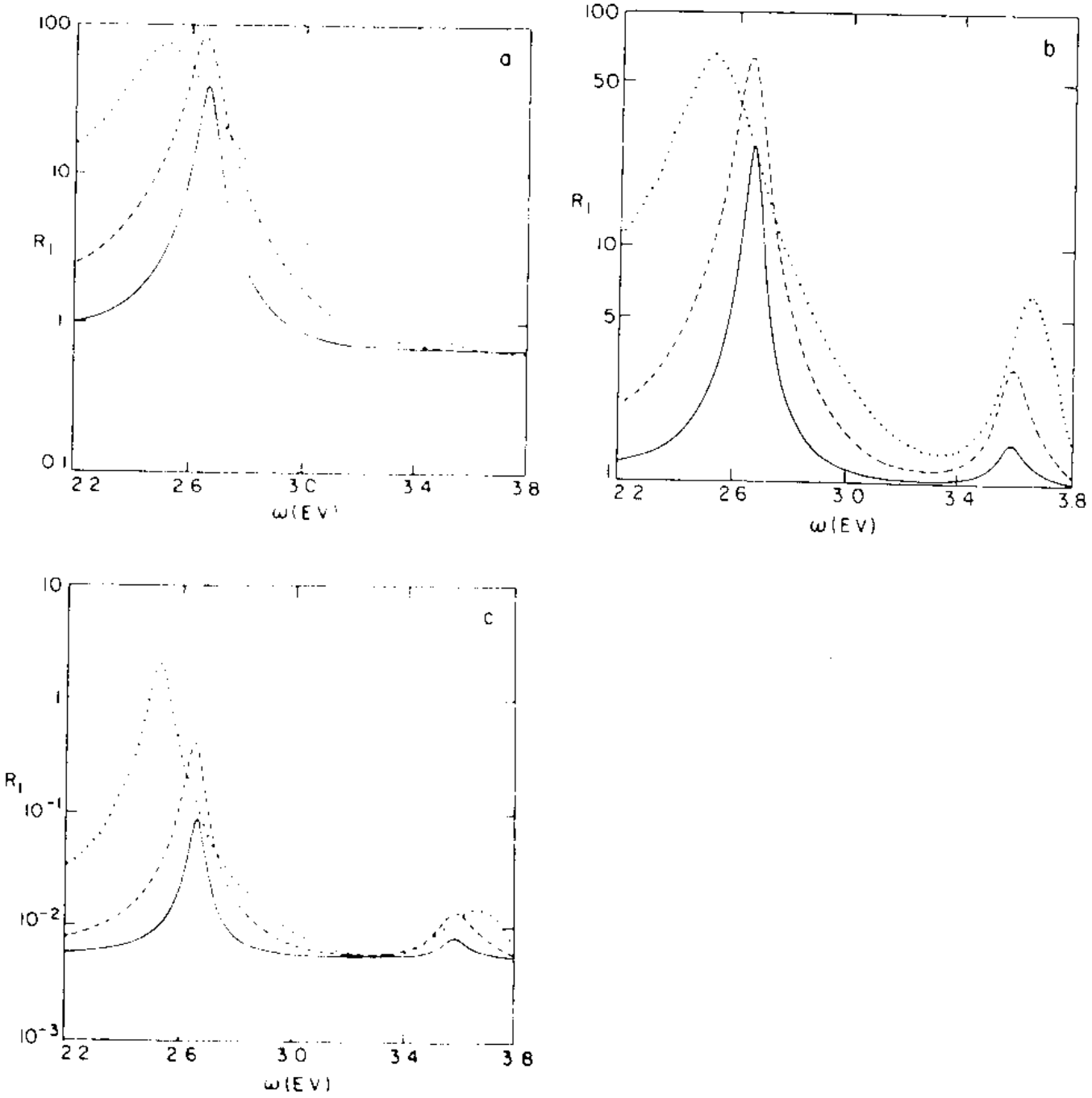

Fig. 8. Same as fig. 7 for films made of oblate spheroids, $\eta = 0.4$. Full line, $n = 3 \times 10^9$ cm^{-2}; dashed line, $n = 1.5 \times 10^{10}$ cm^{-2}, dotted line, $n = 7 \times 10^{10}$ cm^{-2}.

related to the inhomogeneity of the intensity distribution in the film.

The island density dependence of R_1 versus ω is displayed in figs. 7 and 8. Figs. 7a, 7b and 7c (corresponding to incident angles $\varphi_0 = 0°$, 45° and 89° respectively of the p-polarized radiation) show $R_1(\omega)$ for a square array of prolate ellipsoids ($a = 200$ Å, $\eta = a/b = 2.0$) for different island density ($n = 1.0 \times 10^{-6}$, 5×10^{-6} and 2.5×10^{-5} Å^{-2}). Figs. 8a, 8b and 8c show similar results for arrays of oblate spheroids ($a = 100$ Å, $\eta = a/b = 0.4$, $n = 3 \times 10^{-7}$, 1.5×10^{-6}, 7×10^{-6} Å^{-2}). The bulk dielectric function of silver is used for these calculations.

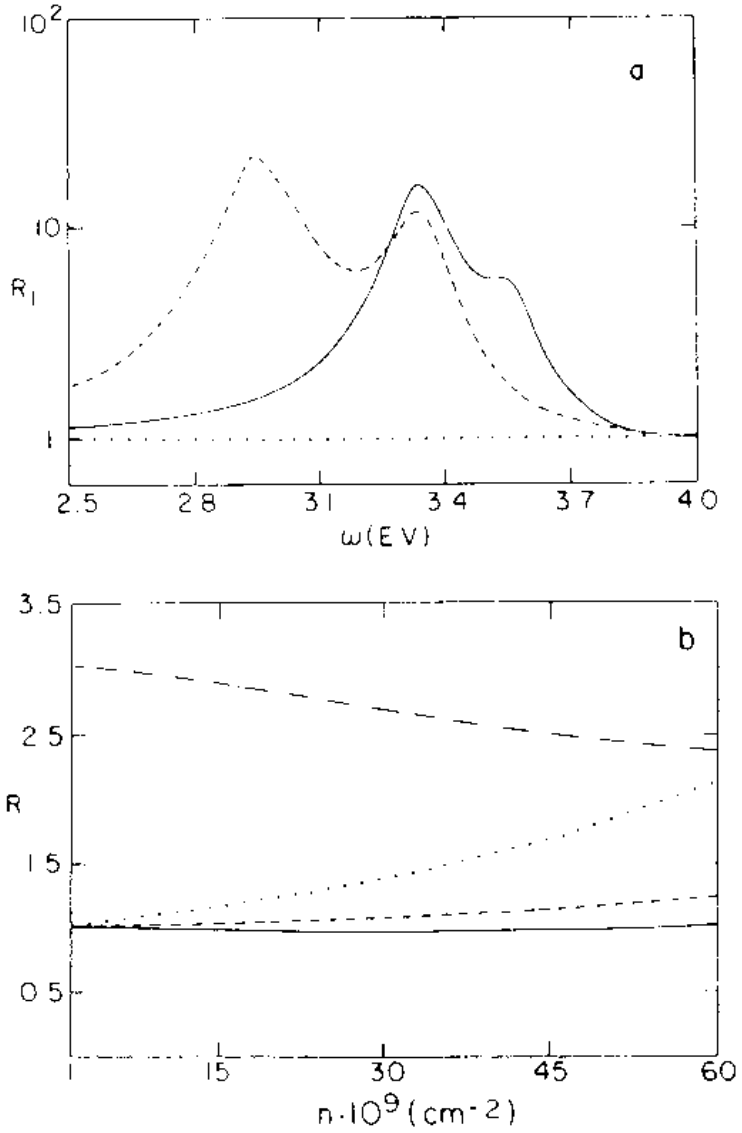

Fig. 9. Enhancement ratio for a film made of a square array of spheroids $\varphi = 45°$ (a) R_1 as a function of ω, $n = 2\times10^{11}$ cm^{-2}, $a = 200$ Å, $b = 100$ Å. The support substrate is quartz. Full line, silver spheroids in vacuum, dashed line, silver spheroids in water, dotted line, perfectly conducting spheroids in vacuum. (b) Enhancement ratio as a function of spheroid density for perfectly conducting spheroids of fixed volume ($V = 10^6$ Å^3) on quartz. Full line, $a = 400$ Å, $\eta = 2.0$; dashed line, $a = 250$ Å, $\eta = 1.0$; dotted line, $a = 160$ Å, $\eta = 0.5$. These results are for R_1, the enhancement averaged over the entire volume between the spheroids. Dash-dotted line, $a = 250$ Å, $\eta = 1.0$, enhancement averaged over shells of thickness $w = 10$ Å around each particle

The sensitivity of the enhancement ratio R_1 to the choice of dielectric functions is studied in fig. 9. Fig. 9a compares $R_1(\omega)$ for silver spheroids ($n = 2\times10^{-5}$ Å^{-2}, $a = 200$ Å, $\eta = 2.0$) on quartz in vacuum ($\varepsilon_0 = \varepsilon_1 = 1.0$) to the same system in water ($\varepsilon_0 = \varepsilon_1 = 1.77$) and to the same system made of perfectly conducting spheroids ($\varepsilon_2 = \infty$) in vacuum. Fig. 9b displays the coverage (n) dependence of R_1 of a sqaure array of perfectly conducting spheroids of fixed volume and different aspect ratios, on quartz in vacuum.

In fig. 10 we compare calculations based on the electrostatic approximation to calculations which take into account retardation effects. In this calculation we use a square lattice of spheres and incident radiation with $\varphi_0 = 0$. It is seen

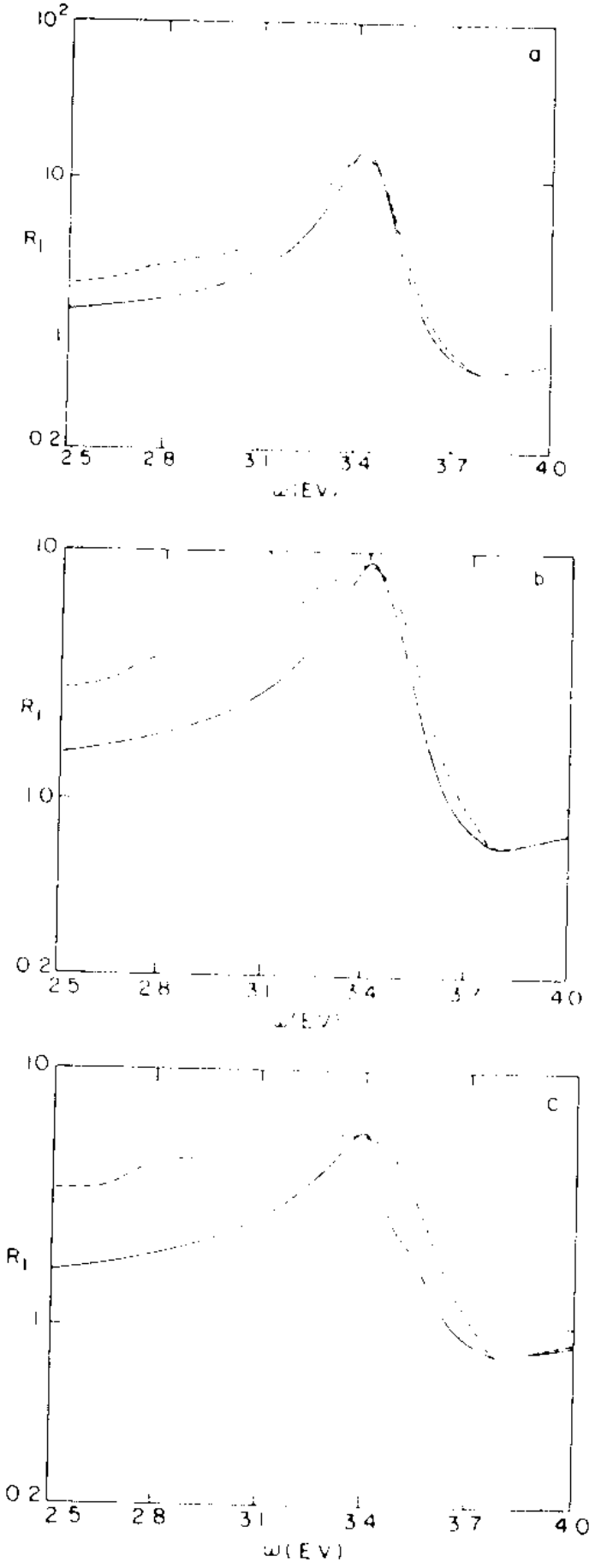

Fig. 10. Enhancement ratio R_l as a function of incident light frequency for a square array of silver spheres (bulk) on quartz. $\varphi = 0°$. Full line, no retardation included; dashed line, retardation taken into account using eq. (3.22). (a) $n = 1.28 \times 10^{11}$ cm^{-2}, $a = 150$ Å; (b) $n = 3.2 \times 10^{10}$ cm^{-2}, $a = 300$ Å; (c) $n = 8 \times 10^{9}$ cm^{-2}, $a = 600$ Å.

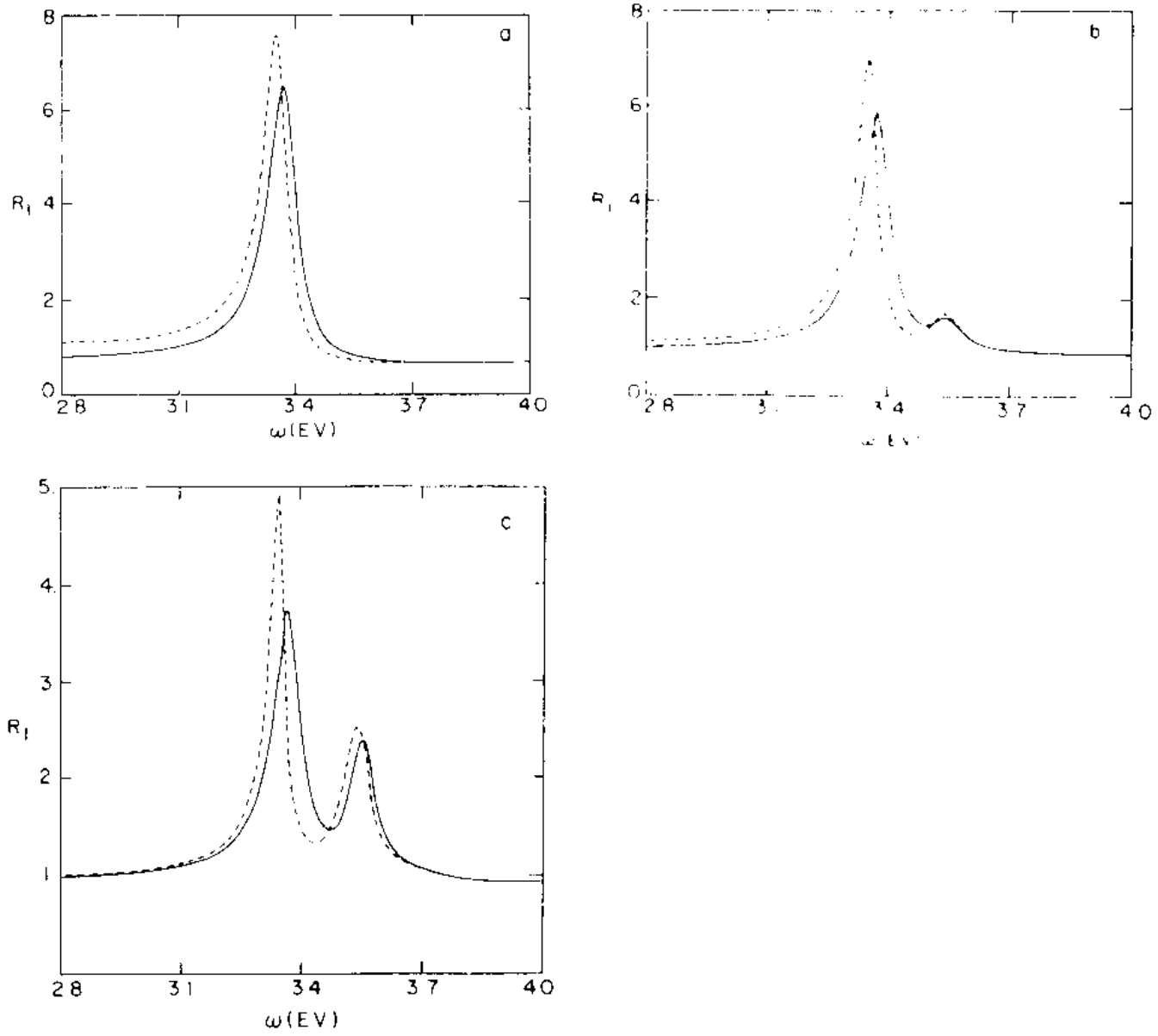

Fig. 11. Enhancement ratio R_1 versus incident light frequency for a square array of silver spheroids (a = 200 Å, η = 0.75, $n = 4.5\times10^{10}$ cm^{-2}, bulk dielectric function of silver) on quartz. Full line, calculation based on the ansatz (3.15); dashed line, calculation based on a self-consistent solution of eqs. (3.7), (3.20) and (3.21). (a) $\varphi = 5°$; (b) $\varphi = 30°$; (c) $\varphi = 60°$

that retardation makes an appreciable effect for lower densities so that the nn distance is larger than $\sim 0.1\lambda_0$.

All the results discussed above are obtained using the ansatz (4.19) for $E_0/\langle E_F\rangle$. Finally in fig. 11 we compare results based on this ansatz to those obtained by solving self-consistently eqs. (3.7), (3.20) and (3.21) for ε_e for the given angle of incidence. We see that the ansatz (4.19) provides a reasonable approximation to the rigorous result in non-resonance situations, while considerable deviations are obtained close to resonance. The deviations increase for higher island densities (which correspond to larger enhancement ratios). However, for high densities we have encountered convergence problems in our self-consistent iteration procedure.

5. Discussion and conclusion

In sections 2-4 we have described a method for evaluating intensity enhancement ratios for the electromagnetic field in composite dielectric films. The calculation relies on several assumptions and approximations which (apart of assumption (a) below) are common in the literature on light scattering from composite films. These are:

(a) The assumed equivalence of the definitions (2.9) and (2.14) of the effective dielectric function of the film. While these two definitions are rigorously equivalent for an infinite three-dimensional composite, this assumption for a thin film is equivalent to the approximation which replaces the potentials on the two film boundaries by their averages over length scales large relative to the characteristic length scale for the film inhomogeneity.

(b) In evaluating the film polarization from the microscopic models of fig. 3 we have assumed that each dielectric grain together with its image constitutes a point dipole. The same assumption was repeated for the evaluation of the image contributions and for the evaluation of the average field in the shells surrounding the grains.

(c) Damping due to finite size effect as well as radiative damping contributions were taken into account using the approximations (4.24) and (4.25) respectively. In some of the calculations these corrections were disregarded altogether and the bulk dielectric function of silver was used for the island diectric response.

(d) The electrostatic approximation has been used for most of the calculations. When we did take account of retardation, we have ignored the conceptual difficulties involved in defining ε_e for a medium whose characteristic length scale of the inhomogeneous structure is not small relative to the radiation wavelength.

(e) We have used the ansatz (3.15) for most of the calculations in evaluating the effective dielectric function for the film, while a more rigorous argument shows that ε_e is not well defined for a thin composite film.

The validity of some of the assumptions and approximations listed above have been tested in the calculations reported in section 4. For islands of sizes between 50 and 500 Å, finite size and radiative damping effects make only a small difference (fig. 4a). Retardation can be disregarded for nearest neighbour distance between the islands small relative to the wavelength (figs. 4b and 10). It should be kept in mind that the theory presented here can be used to estimate average intensity enhancements in composite films where the needed effective dielectric function is obtained from experimental measurements. The results obtained in this way are not sensitive to the approximations mentioned above.

Figs. 5–9 provide some quantitative aspects of intensity enhancement in composite films. It is seen that the average intensity can be enhanced by 1–2

orders of magnitude near the peaks of the "collective resonances" [22] of the film. This is a rather large enhancement ratio considering the fact that this is the enhancement averaged over all the volume outside the dielectric grains. When only thin shells around these grains are considered the corresponding enhancement is a few times larger (fig. 6). It should be noticed that the resonance behaviour (position and width of the peaks) of the intensity averaged over these shells is very similar to that obtained from averaging over the entire volume outside the grains.

While the magnitude of the enhancement changes only modestly on going from an ordered to a random composite film (fig. 5) the resonance behaviour changes drastically. This is seen in fig. 5 for particle shape randomness. The effects of positional randomness are not fully taken into account by the present calculation as discussed in section 3. It should be noticed that further broadening of the resonance behaviour results from retardation effects (fig. 10).

The effect of island density, island shape and of the incident angle is seen from the results displayed in figs. 7 and 8. The following points concerning these results are of interest:

(a) The double peaked nature of the enhancement ratios versus incident frequency corresponds to the excitation of longitudinal and transversal collective resonances [23] in the composite film. The lower frequency peak corresponds to excitation along the longer axis of the ellipsoids making the film.

(b) The larger enhancement ratios obtained for the films made of oblate spheroids ($\eta < 1$), even though for these films (fig. 6) we have taken smaller particle densities than for the prolate spheroid films (fig. 7), are mainly due to the fact that the film thickness d is smaller for the oblate structure. This makes the volume fraction occupied by the spheroids bigger for the same density of particles and the same particle volume. Another reason for the stronger enhancement obtained for the oblate structures is that interaction between oblate grains shifts the longer wavelength peak more to the red (see below) where the imaginary part of the dielectric function of silver is smaller.

(c) It is important to notice that for increasing particle density the two resonance peaks move towards each other and coalesce in the prolate case (fig. 7) while they move away from each other in the oblate case (fig. 8). More specifically the longer wavelength peak moves to the blue for the prolate spheroid film and to the red for the oblate spheroid film. These results are in agreement with the calculations of Burstein et al. [23] on the resonance behaviour of films made of oblate spheroids, as well as with the blue shift usually calculated for molecules adsorbed on a surfade in a perpendicular configuration [24]. It should be mentioned that resonances observed in the incident frequency dependence of surface enhanced Raman scattering are usually red shifted relative to what is expected for a single small substrate particle. However inter-particle interactions are only one factor affecting this shift, the other being the particle size (higher multipole resonances lie on the

red side of the dipolar resonance) and retardation effects. We also note that a double peak behaviour has so far not been observed in SERS experiments on surface island films.

(d) The averaged intensity enhancement ratios depend dramatically on the incident angle. This results from two factors: first the direction of the incident field affects the relative response due to the longitudinal and the transversal modes and, secondly, the incident direction affects the reflection coefficient thus affecting the average field in the film. Thus for glancing incidence ($\varphi = 89°$ in figs. 7 and 8) the reflection coefficient is almost unity and the field practically does not penetrate into the film. This results in the very small values of R_1 obtained for this case. It should be noted that strong incidence angle dependence is observed in SERS measurements [25] in agreement with our results.

The dependence of the enhancement ratios on the dielectric functions of the particles and of the surrounding medium (fig. 9) follows a pattern expected from calculations and experiments involving single dielectric particles [26]. One interesting observation is that for perfectly conducting particles (as silver would practically be at infrared frequencies) the *average* enhancement ratios are very small even though the field is expected to be large near the sharp edges of the spheroids due to the "lightening rod" effect [27].

To end this discussion we comment again on the difficulty involved in defining ϵ_e for a thin composite film. As shown in section 3 a proper calculation of ϵ_e yields a result which depends on the polarization and direction of the incident radiation. This stands in contrast to the usual attempts to determine from ellipsometric measurements a single effective dielectric function characterizing a given composite film. Difficulties associated with such ill-defined effective dielectric function are seen (fig. 11) to arise mainly near the film resonances. Implications of this observation for ellipsometric characterization of thin films will be discussed elsewhere.

In conclusion, we have demonstrated that the local field intensity in thin composite films is considerably enhanced near the collective resonances associated with the film optical response. The enhancement ratios can be as large as 1–2 orders of magnitude even when averaged over the entire volume between the dielectric grains making the film. The effects depends on the dielectric function of the components making the film, as well as on those of the support material and the surrounding medium, on the wavelength, direction and polarization of the incident radiation and on the morphology of the film. This enhancement plays an important role in surface enhanced Raman scattering (calculations involving single dielectric particles [4] indicate that the electromagnetic contribution to the enhancement associated with SERS is related to the square of the enhancement of the field intensity at the location of the adsorbed molecule) as well as in other optical phenomena involving molecules adsorbed on rough dielectric surfaces and on surface island films.

Acknowledgements

This research was supported by grants from the United State-Israel Binational Science Foundation, Jerusalem, Israel, and from the Commission for Basic Research of the Israel Academy of Science. We thank D. Bergman for helpful discussions.

Appendix

Here we outline the calculation of transmission and reflection coefficients of uniaxial films [15] and extract the quantities needed to evaluate the ratio R_1, eq. (2.3). The electric fields associated with the incident, reflected and transmitted waves and with the wave in the film are

$$\boldsymbol{E}_{\mathrm{I}}(\boldsymbol{r},t) = \boldsymbol{E}_{\mathrm{I}} \exp(\mathrm{i}\boldsymbol{k}_{\mathrm{I}} \cdot \boldsymbol{r} - \mathrm{i}\omega t), \tag{A.1}$$

$$\boldsymbol{E}_{\mathrm{R}}(\boldsymbol{r},t) = \boldsymbol{E}_{\mathrm{R}} \exp(\mathrm{i}\boldsymbol{k}_{\mathrm{R}} \cdot \boldsymbol{r} - \mathrm{i}\omega t), \tag{A.2}$$

$$\boldsymbol{E}_{\mathrm{F}}(\boldsymbol{r},,t) = \boldsymbol{E}_{\mathrm{Fd}} \exp(\mathrm{i}\boldsymbol{k}_{\mathrm{Fd}} \cdot \boldsymbol{r} - \mathrm{i}\omega t) + \boldsymbol{E}_{\mathrm{Fu}} \exp(\mathrm{i}\boldsymbol{k}_{\mathrm{Fu}} \cdot \boldsymbol{r} - \mathrm{i}\omega t), \tag{A.3}$$

$$\boldsymbol{E}_{\mathrm{T}}(\boldsymbol{r},t) = \boldsymbol{E}_{\mathrm{T}} \exp(\mathrm{i}\boldsymbol{k}_{\mathrm{T}} \cdot \boldsymbol{r} - \mathrm{i}\omega t). \tag{A.4}$$

We take the optical axis to be in the z direction. The origin for the transmitted wave E_{T} is taken on the FS plane. The origin for all other waves is taken to be on the 0F plane (see fig. 2).

We take the magnetic permeability μ to be unity for all phases, so that for an isotropic medium $N = \sqrt{\varepsilon}$, N being the refraction index and $|\boldsymbol{k}| = N\omega/c$. For a uniaxial medium characterized by $\varepsilon^{\parallel}$ and $\varepsilon^{\perp}$, N depends on the direction and polarization of the electromagnetic wave. For s polarization

$$N(\varphi) = \sqrt{\varepsilon^{\parallel}}, \tag{A.5}$$

independent of direction, while for p polarization

$$N(\varphi) = \left(\frac{\sin^2\varphi}{\varepsilon^{\perp}} + \frac{\cos^2\varphi}{\varepsilon^{\parallel}} \right)^{-1/2}, \tag{A.6}$$

where φ is the angle between the optical axis and the $\boldsymbol{k}$ vector in the medium.

Consider first the reflection and transmission problem for the interface between two semi-infinite uniaxial media a and b (fig. 12), where the interface is perpendicular to both optical axes. All the $\boldsymbol{k}$ vectors are co-planar and the generalized Snell law is

$$\varphi_{\mathrm{I}} = \varphi_{\mathrm{R}}, \quad N_{\mathrm{a}}(\varphi_{\mathrm{I}}) \sin(\varphi_{\mathrm{I}}) = N_{\mathrm{b}}(\varphi_{\mathrm{T}}) \sin(\varphi_{\mathrm{T}}). \tag{A.7}$$

in what follows we write φ_{a} for the incident (reflected) angle $\varphi_{\mathrm{I}} = \varphi_{\mathrm{R}}$ in medium a and φ_{b} for the transmitted angle φ_{T} in medium b.

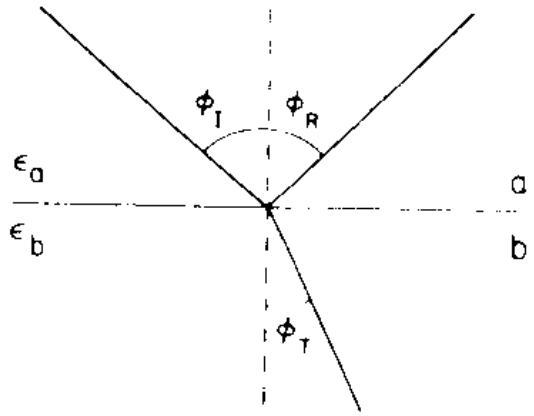

Fig. 12. A schematic description of refraction of reflection of electromagnetic radiation incident on a planar boundary separating two media, establishing the notation used in the appendix. Note that in the text we use $\varphi_a = \varphi_I = \varphi_R$, $\varphi_b = \varphi_T$.

In addition to φ we have to consider, for the p polarization case the (complex) angle χ between the Poynting vector $(c/4\pi)\boldsymbol{E}\times\boldsymbol{H}$ and the optical axis. For an isotropic medium as well as for the s polarization with $\boldsymbol{E}$ perpendicular to the optical axis $\chi = \varphi$. For a uniaxial medium and the p polarization case, χ is given by

$$\sin^2\chi = \frac{\sin^2\varphi}{\sin^2\varphi + \left(\epsilon^{\perp}/\epsilon^{\parallel}\right)^2\cos^2\varphi}. \tag{A.8}$$

We note that for the s polarization case the electric field vector is perpendicular to the optical axis while for the p polarization case the angle between them is $\pi - \chi$.

In terms of φ_a, φ_b, χ_a, χ_b and N_a, N_b ($\chi_{a,b}$ and $N_{a,b}$ are obtained from (A.5)–(A.7) by using φ_a and ϵ_a or φ_b and ϵ_b as needed) we obtain the reflection r_{ab} and transmission t_{ab} coefficients for a wave incident from a on the ab interface in the forms: *s polarization*

$$r_{ab} = \frac{N_a\cos\varphi_a + N_b\cos\varphi_b}{N_a\cos\varphi_a + N_b\cos\varphi_b}, \tag{A.9}$$

$$t_{ab} = \frac{2N_a\cos\varphi_a}{N_a\cos\varphi_a + N_b\cos\varphi_b}. \tag{A.10}$$

p polarization

$$r_{ab} = \frac{\epsilon_b^{\perp}\sin\chi_b}{\epsilon_a^{\perp}\sin\chi_a} - \frac{\cos\chi_b}{\cos\chi_a}\left(\frac{\epsilon_b^{\perp}\sin\chi_b}{\epsilon_a^{\perp}\sin\chi_a} + \frac{\cos\chi_b}{\cos\chi_a}\right)^{-1}, \tag{A.11}$$

$$t_{ab} = 2\left(\frac{\epsilon_b^{\perp}\sin\chi_b}{\epsilon_a^{\perp}\sin\chi_a} + \frac{\cos\chi_b}{\cos\chi_a}\right)^{-1}. \tag{A.12}$$

Next consider the model of fig. 2. The total reflection and transmission coefficients R and T and the coefficients κ_d and κ_u (see fig. 2) may be obtained by considering the multiple reflection–refraction process in the film, in a way identical to that used for isotropic films. The results, when expreseed in terms of the coefficients t_{0F}, t_{F0}, t_{FS}, r_{0F} and r_{FS} are

$$R = \left[r_{0F} + r_{FS}\exp(2i\beta)\right]/\left[1 + r_{0F}r_{FS}\exp(2i\beta)\right], \tag{A.13}$$

$$T = t_{0F}t_{FS}\exp(i\beta)/\left[1 + r_{0F}r_{FS}\exp(2i\beta)\right], \tag{A.14}$$

$$\kappa_d = t_{0F}/\left[1 + r_{0F}r_{FS}\exp(2i\beta)\right], \tag{A.15}$$

$$\kappa_u = \kappa_d r_{FS}\exp(2i\beta), \tag{A.16}$$

where

$$\beta = N_F(\varphi_F)\,(\omega d/c)\cos(\varphi_F). \tag{A.17}$$

Eqs. (A.8) and (A.15)–(A.17) may now be used for the s and p polarization cases by using the particular r and t coefficients from eqs. (A.9)–(A.12) to evaluate the ρ factors of eqs. (2.5) and (2.6).

References

[1] R.K. Chang and T.E. Furtak, Eds., Surface Enhanced Raman Scattering (Plenum, New York, 1982).

[2] R.R. Chance, A. Prock and R. Silby, Advan. Chem. Phys. 37 (1978) 1;
A.M. Glass, P.F. Liao, T.G. Bergman and D.H. Olson, Opt. Letters 5 (1980) 368;
S. Garoff, D.A. Weitz, T.J. Gramila and C.D. Hanson, Opt. Letters 6 (1981) 245;
A. Harstein, J.R. Kirtley and J.C. Tsang, Phys. Rev. Letters 45 (1980) 301;
A. Nitzan and L.E. Brus, J. Chem. Phys. 5 (1981) 2205;
G.M. Goncher and C.B. Harris, J. Chem. Phys. 77 (1982) 3767;
D.A. Weitz, S. Garoff, J. Gersten and A. Nitzan, The Enhancement of Raman Scattering, Resonance Raman Scattering and Fluorescence from Molecules Adsorbed on Rough Silver Surfaces, submitted.

[3] S.L. McCall and P.M. Platzman, Phys. Rev. B22 (1980) 1660;
F.W. King and G.C. Schatz, Chem. Phys. 38 (1979) 245;
Ph. Avouris and J.E. Demuth, J. Chem. Phys. 75 (1981) 4783;
D. Schmeisser, J.E. Demuth and Ph. Avouris, Chem. Phys. Letters 87 (1982) 324;
A. Otto, I. Pockrand, J. Billman and C. Pettenkofer in ref [1];
B.N.J. Persson, Chem. Phys. Letters 82 (1981) 561.

[4] (a) J. Gersten and A. Nitzan, J. Chem. Phys. 73 (1980) 3023, 75 (1981) 1139;
M. Kerker, D.S. Wang and H. Chew, Appl. Opt. 19 (1980) 2256;
D.S. Wang and M. Kerker, Phys. Rev. B24 (1981) 1777;
S.L. McCal, P.M. Platzman and P.A. Wolf, Phys. Letters A77 (1980) 381
(b) P.K. Aravind, A. Nitzan and H. Metiu, Surface Sci. 110 (1981) 189;
M. Inoue and K. Ohtaka, in Proc. SERS Symp., Ed. H. Ueda (Tokyo, 1981).
(c) S.S. Jha, J.R. Kirtley and T.C. Tsang, Phys. Rev. B22 (1980) 3973, Solid State Commun. 35 (1980) 509; P.K. Aravind and H. Metiu, Surface Sci. 109 (1980) 95.

[5] See, e.g., R.M.A. Azzam and N.M. Bashara, Ellipsometry and Polarized Light (North-Holland, Amsterdam, 1977).
[6] For reviews of the Maxwell-Garnett (or Clausius–Mossotti) approximation as well as other simple approximations for the effective dielectric function see, e.g., R. Landauer, in: Electrical Transport and Optical Properties of Inhomogeneous Media, AIP Conf. Proc. No. 40, Eds. J.C. Garland and D.B. Tanner (American Inst. of Phys., New York, 1978).
[7] D.J. Bergman and A. Nitzan, Chem. Phys. Letters 88 (1982) 409.
[8] D.E. Aspnes, Phys. Rev. Letters 48 (1982) 1629.
[9] This picture is implicit in the method which uses an expression, eq. (2.8), for ϵ_e which is valid for such a geometry (see Bergman, ref. [10]).
[10] D.J. Bergman, Phys. Rept. 43 (1978) 377.
[11] S. Yoshida, T. Yamaguchi and A. Kinbara, J. Opt. Soc. Am. 61 (1971) 62;
T. Yamaguchi, S. Yoshida and A. Kinbara, Thin Solid Films 18 (1973) 63; 21 (1974) 173; J. Opt. Soc. Am. 64 (1974) 1563.
[12] M.J. Dignam and M. Moskovits, JCS Faraday II, 69 (1973) 56.
[13] O. Hunderi, Surface Sci. 96 (1980) 1, and references therein.
[14] U. Laor and G.C. Schatz, J. Chem. Phys. 76 (1982) 2888; Chem. Phys. Letters 83 (1981) 566.
[15] L.P. Mosteller and J.F. Wooten, J. Opt. Soc. Am. 58 (1968) 511;
M.J. Dignam, M. Moskovits and R.W. Stobie, Trans. Faraday Soc. 67 (1971) 3306.
[16] Z. Kotler and A. Nitzan, J. Phys. Chem. 86 (1982) 2011. Even though this paper considers a single sphere the result, eq. (2.20), is correct for any number of interacting spheres as long as the field within the sphere under consideration may be assumed to be homogeneous. This assumption is identical to taking the dielectric grains as point dipoles for evaluating the effect of their mutual interactions.
[17] Here we assumed that the dielectric function in the shell is identical to that in the rest of the medium between the dielectric grains. A more general result can be easily derived (see, e.g., Kotler and Nitzan in ref. [16]).
[18] The factor g^δ does not appear in refs. [11] or [12] and arises here because the induced dipole calculated from eq. (3.3) with the polarizabilities (3.1) includes the sum of the actual dipole and its image in the substrate. The latter is eliminated by multiplying by the factor g^δ.
[19] As seen in section 4 (fig. 12) the effect is most pronounced near the film resonance.
[20] In evaluating the lattice sum of the r_{jA}^{-1} terms we have summed numerically over a few (~ 20) nearest neighbour shells and converted the rest of the sum into an integral using $\int_A^\infty d^3r \exp(ikr) = -\exp(ikA)/ik$.
[21] A. Wokaun, J.P. Gordon and P.F. Liao, Phys. Rev. Letters 48 (1982) 957.
[22] F.P. Marton and J.R. Lemon, Phys. Rev. B4 (1971) 271;
F.P. Marton and J.R. Lemon, Phys. Rev. B15 (1977) 1719;
D.G. Goad and M. Moskovits, J. Appl. Phys. 49 (1978) 2929;
M. Moskovits, J. Chem. Phys. 69 (1978) 4159.
[23] E. Burstein and C.Y. Chen, in: Proc. 7th Intern. Conf. on Raman Spectroscopy, Ottawa, 1980;
C.Y. Chen, E. Burstein and S. Lundqvist, Solid State Commun. 32 (1979) 63;
C.Y. Chen, E. Burstein and S. Lundqvist, in: Proc. US–USSR Symp. on Inelastic Light Scattering in Solids, Eds. J.L. Birman, H.Z. Cummins and K.K. Rebane (Plenum, New York, 1979).
[24] See, e.g., R.M. Hammaker, S.A. Francis and R.P. Eischens, Spectrochim. Acta 21 (1965) 1295;
G.D. Mahan and A.A. Lucas, J. Chem. Phys. 68 (1978) 1344;
M. Moskovits and J.E. Hulse, Surface Sci. 78 (1978) 397.
[25] B. Pettinger, U. Wenning and H. Wetzel, Chem. Phys. Letters 67 (1979) 192;
G.R. Trott and T.E. Furtak, Solid State Commun. 36 (1980) 1101.

[26] P.F. Liao, J.G. Bergman, D.S. Chemla, A. Wokaun, J. Melngailis, A.M. Hawryluk and E.P. Econumou, Chem. Phys. Letters 82 (1981) 355.
[27] J.I. Gersten, J. Chem. Phys. 72 (1980) 5779.